Chapter 6

Binaries and stellar evolution

In the next few chapters we will consider evolutionary processes that occur in binary stars. In particular we will address the following questions: (1) Which kinds of interaction processes take place in binaries, and how do these affect their evolution as compared to that of single stars? (2) How do observed types of binary systems fit into the binary evolution scenario?

One type of interaction process was already treated in Chapter 5,[1] namely the dissipative effect of tides which can lead to spin-orbit coupling and to long-term evolution of the orbit (semi-major axis a and eccentricity e). Tidal interaction does not directly affect the evolution of the stars themselves, except possibly through its effect on stellar rotation. In particular it does not change the masses of the stars. However, when in the course of its evolution one of the stars fills its critical equipotential surface, the Roche lobe (Sect. 3.4), mass transfer may occur to the companion, which strongly affects both the masses and evolution of the stars as well as the orbit. Before treating mass transfer in more detail, in this chapter we briefly introduce the concept of Roche-lobe overflow, and give an overview of the aspects of single-star evolution that are relevant for binaries.

6.1 Roche-lobe overflow

The concept of *Roche-lobe overflow* (RLOF) has proven very powerful in the description of binary evolution. The critical equipotential surface in the Roche potential, passing through the inner Lagrangian point L_1, define two Roche lobes surrounding each star (Sect. 3.4). We can define an equivalent radius of the Roche lobe as the radius of a sphere with the same volume, $V_\mathrm{L} = \frac{4}{3}\pi R_\mathrm{L}^3$. Eq. (3.35) provides a fitting formula for the Roche radius of *1 that is accurate to better than 1 % over the entire range of mass ratios $q = M_1/M_2$, i.e.

$$\frac{R_{\mathrm{L},1}}{a} = \frac{0.49q^{2/3}}{0.6q^{2/3} + \ln(1 + q^{1/3})} \tag{6.1}$$

We will often use a somewhat less accurate but simpler fitting formula that is valid for $0.1 < q < 10$:

$$\frac{R_{\mathrm{L},1}}{a} \approx 0.44\frac{q^{0.33}}{(1 + q)^{0.2}} \tag{6.2}$$

Both these expressions are due to P. Eggleton.

Hydrostatic equilibrium in the corotating frame requires that the stellar surface coincides with an equipotential surface. This allows three possible configurations in which both stars are in hydrostatic equilibrium, all of which are observed to occur in nature:

[1] i.e., the articles by Hut (1980, 1981) and Verbunt (2007).

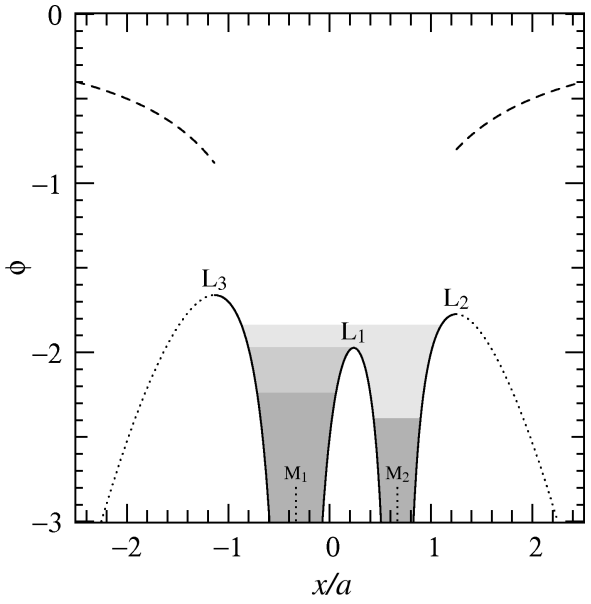

Figure 6.1. Shape of the Roche potential (solid line) along the line connecting the two stars, for a binary with mass ratio $q = M_1/M_2 = 2$. The horizontal scale is in units of the semi-major axis a, and the potential ϕ is in units of $G(M_1 + M_2)/a$. The locations of the centres of mass of the two stars are indicated by M_1 and M_2, and the Lagrangian points by L_1, L_2 and L_3. Gray scales indicate the three possible stable binary configurations: detached (dark), semi-detached (middle) and contact (light gray).

Matter located outside L_2 and L_3 cannot maintain corotation with the orbit, and the Roche potential (shown as dotted lines) loses its physical meaning. Such matter is still bound to the system, as indicated by the dashed lines that represent the gravitational potential of the binary at large distance.

- In a *detached binary* both stars fill an equipotential surface inside their Roche lobes. In this case their structure and evolution is not much affected by the Roche geometry, and can be well approximated by that of single stars.

- If one of the stars exactly fills its Roche lobe while the other is still smaller, the binary is *semi-detached*. If it grows any larger in size the star encounters a 'hole' in its surface equipotential near L_1. This means that hydrostatic equilibrium is no longer possible in the vicinity of the inner Lagrangian point and matter must flow through the nozzle around L_1 into the Roche lobe of its companion (see Chapter 7). This is the idea behind Roche-lobe overflow.

- A final possibility is where both stars fill the same equipotential surface, at a value of the potential above that of L_1 but below that of the outer Lagrangian point L_2 (Fig. 6.1). Such a configuration is known as a *contact binary*, since it requires the stars to be in physical contact. This means that the stars can exchange heat as well as mass, as indeed appears to be the case in observed contact binaries (see a later chapter).

Binaries start out in a detached configuration. As a result of evolution, i.e. expansion due to nuclear evolution of the stars, possibly combined with orbital shrinking owing to angular momentum loss, $R_1/R_{\rm L,1}$ and $R_2/R_{\rm L,2}$ increase with time. A detached binary can thus evolve into a semi-detached binary or, if both stars fill their Roche lobes, into a contact binary.

Three assumptions are made in the Roche geometry (Sect. 3.4), and it is important to reassess them in the context of binary evolution. First, the gravitational fields of both stars are assumed to be those of point masses. This is reasonable, even when stars are filling their Roche lobes, because most stars are very centrally concentrated. Second, the orbit is assumed to be circular. Third, the stellar rotation is assumed to be synchronized with the orbital motion, since the Roche geometry only applies to matter that corotates with the orbit. These last two assumptions are certainly not generally valid, but they are usually satisfied when stars are close to filling their Roche lobes. The reason is that tidal interaction becomes very effective due to its strong dependence on R/a, e.g. in the equilibrium-tide model the circularization timescale depends on $(R/a)^{-8}$ and the synchronization timescale on $(R/a)^{-6}$ (Chapter 5). Both timescales normally become smaller than the stellar expansion timescale when R is close to $R_{\rm L}$.

6.2 Aspects of single-star evolution

6.2.1 Overview

(Adapted from Tauris & van den Heuvel, 2006, Sec. 16.3)

The evolution of a star is driven by a rather curious property of a self-gravitating gas in hydrostatic equilibrium, which is described by the virial theorem. The radiative loss of energy of such a gas sphere causes it to contract and thereby, due to release of gravitational potential energy, to increase its temperature. Thus, while the star tries to cool itself by radiating away energy from its surface, it gets hotter instead of cooler: a star can be said to have a negative heat capacity. The more it radiates to cool itself, the more it will contract, the hotter it gets and the more it is forced to go on radiating. Clearly, this virial cycle is an unstable situation in the long run and explains why a star that starts out as an extended interstellar gas cloud, must finally end its life as a compact object. In the meantime the star spends a considerable amount of time in intermediate stages, during which the radiative energy loss from its surface is compensated by nuclear energy production in its interior, temporarily halting the contraction – a state known as thermal equilibrium. These long-lived stages are known as the main sequence in the case of hydrogen fusion, the horizontal branch in the case of helium fusion, etc. It is important to realize, however, that stars do *not* shine because they are burning nuclear fuel. They shine because they are hot due to their history of gravitational contraction.

Stars that start out with masses $M \lesssim 8\,M_\odot$ suffer from the occurrence of electron degeneracy in their cores at a certain point of evolution. Since for a degenerate gas the pressure depends only on density and not on the temperature, the ignition of a nuclear fuel will not lead to a stabilizing expansion and subsequent cooling. Instead, the sudden temperature rise due to the liberation of energy after ignition causes a runaway nuclear energy production in a so-called 'flash'. In stars with $M \lesssim 2\,M_\odot$ (low-mass stars) the helium core becomes degenerate during hydrogen shell burning on the giant branch and, when its core mass $M_{\rm He}$ reaches $0.47\,M_\odot$, helium ignites with a flash. The helium flash is, however, not violent enough to disrupt the star and it is followed by steady helium burning. Stars with masses in the range $2 \lesssim M/M_\odot \lesssim 8$ (intermediate-mass stars) ignite helium non-degenerately and non-violently. Both low-mass and intermediate-mass stars develop degenerate carbon-oxygen cores after helium burning. Observations of white dwarfs in Galactic clusters that still contain stars as massive as $8^{+3}_{-2}\,M_\odot$ (e.g. Weidemann, 1990) indicate that such massive stars still terminate their life as a white dwarf. They shed their envelopes by a strong stellar wind on the asymptotic giant branch before carbon has a chance to ignite violently.

Table 6.1. End products of stellar evolution as a function of stellar mass, for single stars and for components of close binary stars (roughly, those undergoing case B mass transfer). The columns 'He-core mass' give the maximum mass of the helium core reached by a star of the given initial mass range, for single and close binary stars. The values given are only indicative, and depend on the metallicity (assumed to be solar) and uncertainties in mass loss rates and convective overshooting (mild overshooting was assumed). For binary stars, they also depend on the orbital period and mass ratio.

	single star		close binary star	
initial mass	He-core mass	final remnant	He-core mass	final remnant
$\lesssim 2.0\,M_\odot$	$\approx 0.6\,M_\odot$	CO white dwarf	$< 0.47\,M_\odot$	He white dwarf
$2.0 - 6\,M_\odot$	$0.6 - 1.7\,M_\odot$	CO white dwarf	$0.4 - 1.3\,M_\odot$	CO white dwarf
$6 - 8\,M_\odot$	$1.7 - 2.2\,M_\odot$	ONe white dwarf	$1.3 - 1.7\,M_\odot$	CO white dwarf
$8 - 10\,M_\odot$	$2.2 - 3.0\,M_\odot$	neutron star	$1.7 - 2.2\,M_\odot$	ONe white dwarf
$10 - 25\,M_\odot$	$3.0 - 10\,M_\odot$	neutron star	$2.2 - 8\,M_\odot$	neutron star
$\gtrsim 25\,M_\odot$	$> 10\,M_\odot$	black hole	$> 8\,M_\odot$	neutron star/black hole

A massive star ($M \gtrsim 8\,M_\odot$) evolves through all cycles of nuclear burning alternating with stages of core contraction after exhaustion of nuclear fuel until its core is made of iron, at which point further fusion requires, rather than releases, energy. The core mass of such a star becomes larger than the Chandrasekhar limit, the maximum mass possible for an electron-degenerate configuration ($\approx 1.4\,M_\odot$). Therefore the core implodes to form a neutron star or black hole. The gravitational energy released in this collapse (4×10^{53} erg $\approx 0.15 M_{\rm core} c^2$) is much larger than the binding energy of the stellar envelope, causing the collapsing star to violently explode and eject the outer layers of the star, with a speed of $\sim 10^4$ km/s, in a supernova event. The final stages during and beyond carbon burning are very short-lived ($\lesssim 10^3$ yr) because most of the nuclear energy generated in the interior is liberated in the form of neutrinos which freely escape without interaction with the stellar gas, thereby lowering the outward pressure and accelerating the contraction and nuclear burning.

The possible end-products and corresponding initial masses are listed in Table 6.1. It should be noted that the actual values of the different mass ranges are only known approximately due to considerable uncertainty in our knowledge of the evolution of massive stars. Causes of this uncertainty include limited understanding of the mass loss undergone by stars in their various evolutionary stages. Another fundamental problem is understanding convection, in particular in stars that consist of layers with very different chemical composition. Finally, there is the unsolved question of whether or not the velocity of convective gas cells may carry them beyond the boundary of the region of the star which is convective according to the Schwarzschild criterion. For example, inclusion of this so-called overshooting in evolutionary calculations decreases the lower mass limit for neutron star progenitors (moderate overshooting was assumed in calculating the values in Table 6.1).

Stars in close binary systems can lose their envelope as a result of mass transfer via Roche-lobe overflow, as we shall see in the following chapters. This is the reason why in close binary systems the lower initial mass limits for producing a certain type of remnant are somewhat larger than for an isolated star. Note, however, that the values quoted in Table 6.1 are only indicative and also depend on the orbital period and mass ratio of the binary.

6.2.2 Stellar time scales

Three time scales associated with single stars are important for the study of binary evolution. In order of increasing length these are:

the dynamical time scale This is the time scale on which a star counteracts a perturbation of its hydrostatic equilibrium. It is given by the ratio of the radius of the star R and the average sound velocity of the stellar matter $c_{\rm s}$:

$$\tau_{\rm dyn} = \frac{R}{c_{\rm s}} \approx 0.04 \left(\frac{M_\odot}{M}\right)^{1/2} \left(\frac{R}{R_\odot}\right)^{3/2} \text{ day} \tag{6.3}$$

the thermal or Kelvin-Helmholtz time scale This is the time scale on which a star reacts when energy loss and energy production are no longer in equilibrium. It is given by the ratio of the thermal energy content of the star $E_{\rm th}$ and the luminosity L:

$$\tau_{\rm KH} = \frac{E_{\rm th}}{L} \approx \frac{GM^2}{2RL} \approx 1.5 \times 10^7 \left(\frac{M}{M_\odot}\right)^2 \frac{R_\odot}{R} \frac{L_\odot}{L} \text{ yr} \tag{6.4}$$

the nuclear time scale This is the time scale on which a star uses its nuclear fuel. It is given by the product of the available fusable matter $M_{\rm core}$ and the fusion energy per unit mass Q, divided by the stellar luminosity. For hydrogen fusion with $Q = 0.007c^2$, this is:

$$\tau_{\rm nuc} = 0.007 \frac{M_{\rm core} c^2}{L} \approx 10^{10} \frac{M}{M_\odot} \frac{L_\odot}{L} \text{ yr} \tag{6.5}$$

In the course of its evolution, a star fuses hydrogen in its core on the nuclear time scale. During this time, on the main sequence, the star does not change its radius very much. On the main-sequence we can use the following mass-radius and mass-luminosity relations in eqs. (6.3–6.5):

$$\frac{R}{R_\odot} \simeq \left(\frac{M}{M_\odot}\right)^{0.7} \tag{6.6}$$

$$\frac{L}{L_\odot} \simeq \left(\frac{M}{M_\odot}\right)^{3.8} \tag{6.7}$$

6.2.3 Evolution of the stellar radius and cases of mass transfer

Fig. 6.2a shows evolution tracks in the Hertzsprung-Russell diagram for stars with masses between 1.0 and 25 $M_\odot$, together with lines of constant radius. For three masses (representing low-mass stars, intermediate-mass stars and massive stars, respectively) the corresponding variation of the stellar radius with time is depicted in Fig. 6.2b-d. During the main sequence (central hydrogen burning) phase all stars show a mild increase in radius. Low-mass stars (e.g. the 1.6 $M_\odot$ star) subsequently expand strongly but relatively slowly – on the nuclear timescale of hydrogen-shell burning – during the ascent of the first giant branch, where they develop degenerate helium cores that grow in mass until the occurrence of the helium flash when the core mass $M_c \approx 0.47\,M_\odot$. In contrast, intermediate-mass stars (e.g. the 4 $M_\odot$ star) expand much more rapidly – on a thermal timescale – as they cross the Hertzsprung gap, before they ignite helium non-degenerately. During helium burning low- and intermediate-mass stars describe a loop in the H-R diagram, and their radius remains smaller than it was at the tip of the giant branch. After helium exhaustion in the centre the radius increases again on the asymptotic giant branch, where such stars develop degenerate carbon-oxygen cores. Massive stars (e.g. the 16 $M_\odot$ star) expand more strongly as they cross the Hertzsprung gap and, at least up to about 25 $M_\odot$, burn helium as a red supergiant while their radius keeps expanding slightly. Even more massive stars experience such strong mass loss that their hydrogen-rich envelope is removed by the time helium ignites; their radius decreases and they become Wolf-Rayet stars.

Based on the variation of the stellar radius with time, three cases of mass transfer can be distinguished. An evolving star in a binary can fill its Roche lobe for the first time as it expands on the main sequence (Case A), as it expands after hydrogen exhaustion (Case B), or as it expands after helium exhaustion (Case C). This is depicted in Fig. 6.2b-d for three different masses. Which of the three cases applies depends on the size of the Roche lobe, which in turn depends on the separation between the two stars and (to a lesser extent) on the mass ratio (see eq. 6.1 or 6.2).

The distinction between cases A, B and C contains information about the evolution state of remnant of the donor after mass transfer. Just as important however is a distinction based on the stability of mass transfer. This depends crucially on whether the donor has a radiative or a convective envelope, as will be discussed in Sect. 7.3. The radius at which stars reach the red giant branch and develop a deep convective envelope is also indicated in Fig. 6.2.

Core mass-radius relation for low-mass giants

Low-mass stars on the first giant branch have degenerate helium cores and their luminosity is generated entirely by hydrogen-shell burning around the growing core. The envelope is so extended that it exerts negligible pressure on the dense core, and the luminosity depends only on the mass of the core: low-mass giants follow a very tight core mass-luminosity relation. These stars have deep convective envelopes and are forced to evolve along a Hayashi line[2] at almost constant effective temperature, which only weakly

[2]The Hayashi line is an almost vertical line in the H-R diagram at $T_{\rm eff} \sim 3000$–5000 K that connects fully convective stellar configurations of a certain mass. A star in hydrostatic equilibrium cannot have an effective temperature smaller than that of the

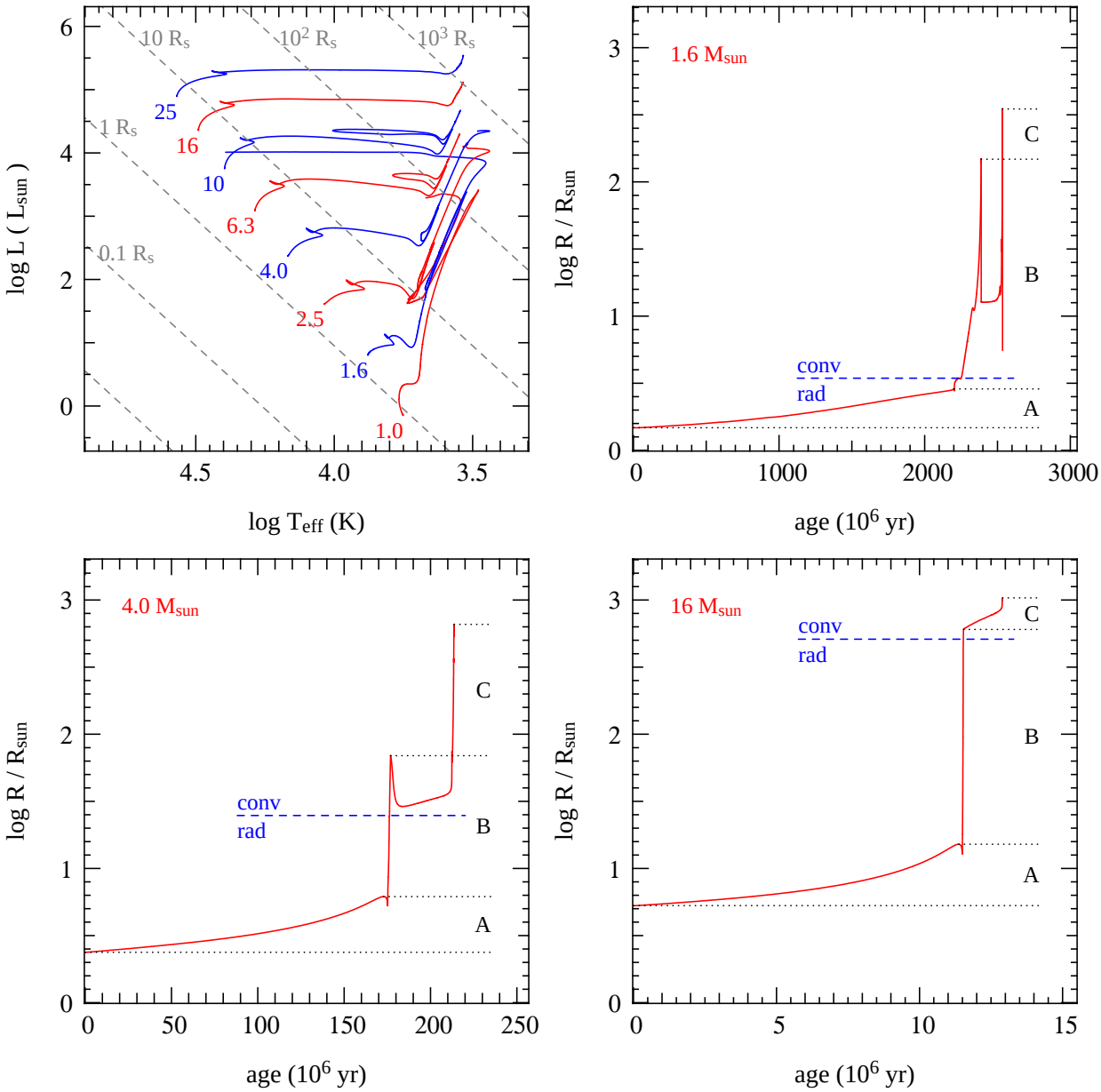

Figure 6.2. Evolution in the H-R diagram (panel a) of single stars with masses between 1.0 and 25 $M_\odot$, as indicated, together with lines of constant radii (in solar radii, dashed lines). The other panels show the variation of the radii of stars of (b) 1.6 $M_\odot$, (c) 4 $M_\odot$ and (d) 16 $M_\odot$ between the ZAMS and either the end of the AGB (1.6 and 4 $M_\odot$) or carbon burning (16 $M_\odot$). The models have been calculated for a metallicity $Z = 0.02$ and a moderate amount of overshooting. The dotted lines indicate the radii at the ZAMS, the end of the MS, the ignition of He, and the maximum radius. The dashed blue line shows the radius at which the stars develop a deep convective envelope on the giant branch.

depends on the mass of the star. Hence there is also a fairly tight core- mass radius relation, as depicted in Fig. 6.3. This relation is very important for low-mass X-ray binaries and certain binary radio pulsars, as we shall see in Chapter 11.

The core-mass radius relation breaks down for masses $\gtrsim 2\,M_\odot$ (the highest mass indicated in Fig. 6.3, as a solid line) and for core masses $\gtrsim 0.47\,M_\odot$ when the radius shrinks in response to helium burning.

Hayashi line appropriate for its mass.

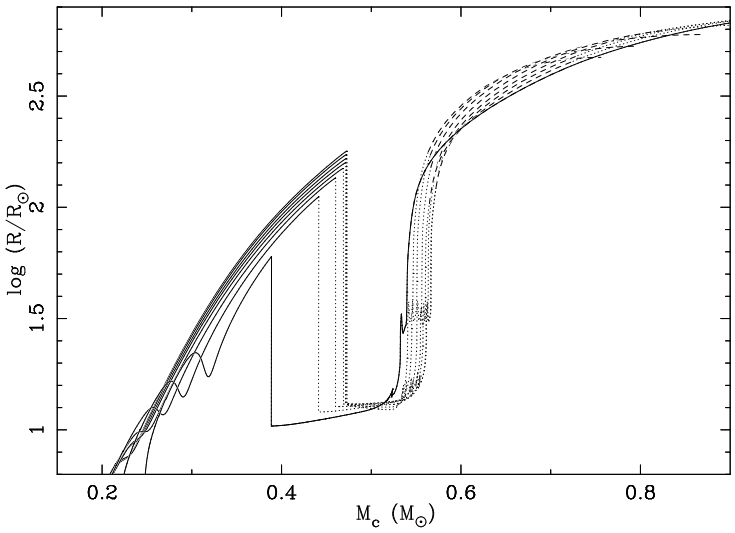

Figure 6.3. Core mass-radius relations for low-mass stars, from detailed stellar models with masses between 0.9 and 2.0 $M_\odot$ computed by van der Sluys et al. (2006). The solid lines correspond to the first giant branch when these stars have a degenerate helium core. The dashed lines show the asymptotic giant branch, with a degenerate carbon-oxygen core. The dotted lines correspond to the core helium-burning phase, when the stellar radius is smaller than the maximum reached on the first giant branch, and during which such stars cannot fill their Roche lobes.

However, for $M_\mathrm{c} \gtrsim 0.6\,M_\odot$ low-mass stars again follow a core mass-radius relation on the asymptotic giant branch.

Exercises

6.1 Show that the ratio of the Roche-lobe radii of binary components is given approximately by

$$\frac{R_{\mathrm{L},1}}{R_{\mathrm{L},2}} \approx q^{0.46} \tag{6.8}$$

for $q = M_1/M_2$ lying between 0.1 and 10.

6.2 For semi-detached binaries there is a relation between the orbital period and the average density of the Roche-lobe filling component, as follows:

$$P = F\left(\frac{\bar{\rho}}{\bar{\rho}_\odot}\right)^{-1/2} \qquad \text{with} \qquad F \approx 0.35\,\mathrm{d}\left(\frac{2}{1+q}\right)^{0.2}, \tag{6.9}$$

where F only depends very weakly on the mass ratio, and can be considered a constant (0.35 d) for practical purposes.

(a) Derive this relation.

(b) Certain 'ultra-compact' binaries have orbital periods of less than 20 minutes. Compare their average density to that of:
- normal main-sequence (MS) stars,
- low-mass helium MS stars, entirely composed of helium, which follow a mass-radius relation $R/R_\odot \approx 0.2(M/M_\odot)$ and have a mass of at least 0.3 $M_\odot$, the minimum mass for helium burning.

(c) What can you conclude about the evolution state of the mass donor in such ultra-compact systems?

6.3 Fig. 6.2c shows how the radius of a star of 4 $M_\odot$ changes during its evolution. Assume such a star has a binary companion of 3 $M_\odot$. Use this plot to calculate:

(a) for which range of orbital periods does mass transfer occur according to case A, case B or case C (determine the transition radii as accurately as possible);

(b) for which orbital periods does the donor star have a radiative envelope.

Chapter 7

Mass transfer in binary stars

A binary system starts out as detached, with both stars in hydrostatic equilibrium and filling an equipotential surface inside their Roche lobes. As a result of evolution, i.e. expansion due to nuclear evolution of the stars, possibly combined with orbital shrinking owing to angular momentum loss, $R_1/R_{\rm L,1}$ and $R_2/R_{\rm L,2}$ increase with time. When one of the stars (usually the most massive star since it has the shortest nuclear timescale) fills its Roche lobe, it encounters a 'hole' in its surface equipotential near L_1. This means that hydrostatic equilibrium is no longer possible in the vicinity of the inner Lagrangian point and matter must flow through the nozzle around L_1 into the Roche lobe of its companion. This is the idea behind Roche-lobe overflow.

In a binary, both stars (*1 and *2) can fill their Roche lobes at subsequent evolutionary stages. We use the convention where *1 denotes the *initially* more massive star of the binary, and *2 the originally less massive star. In this convention the initial mass ratio $q = M_1/M_2 > 1$. During phases of mass transfer we denote the mass-losing star, the *donor*, with subscript 'd' and the companion star, the *accretor*, with subscript 'a' (even if it turns out there is effectively very little or no accretion taking place). Hence the donor can be either *1 or *2, depending on the phase of evolution, but during the first mass transfer phase the donor will always be *1.

7.1 The rate of mass transfer by Roche-lobe overflow

Mass flow through the inner Lagrangian point is, in all its generality, a rather complicated hydrodynamical problem. In the following we will make it plausible that the rate of mass transfer through L_1 depends very sensitively on the fractional radius excess of the donor, $\Delta R/R_{\rm L} = (R_{\rm d} - R_{\rm L})/R_{\rm L}$. This allows a great simplification of the problem in many practical applications.

The rate of mass flow $\dot{M}$ can be written as the product of the density ρ and the velocity v of the gas at L_1, and the cross section S of the stream,

$$\dot{M} \approx (\rho v)_{L_1} \cdot S \tag{7.1}$$

To estimate S consider the Roche potential in the plane through L_1 perpendicular to the line connecting both stars, i.e. in the plane $x = 0$. In the vertical (y) direction the potential has a roughly parabolic shape as follows from the Taylor expansion

$$\Delta\phi \equiv \phi(x,y) - \phi(x,0) = \frac{\partial\phi}{\partial y}\Big|_{L_1} y + \tfrac{1}{2}\frac{\partial^2\phi}{\partial y^2}\Big|_{L_1} y^2 \tag{7.2}$$

$$\approx \tfrac{1}{2}\omega^2 y^2 \tag{7.3}$$

The first derivative of ϕ is zero since $(x,y) = (0,0)$ corresponds to a saddle point in the potential. Furthermore it can be shown, from the definition of the Roche potential in combination with Kepler's law,

that to within a factor of order unity $(\partial^2\phi/\partial y^2)|_{L_1} \approx \omega^2$ where ω is the orbital frequency, which gives the second equation. This is interpreted as follows: the amount $\Delta\phi$ by which the surface potential of the donor exceeds the critical potential, is approximately ω^2 times the cross section y^2 of the stream passing through L_1. By considering a point on the surface of the donor far away from L_1, where the potential is roughly spherical and dominated by the gravitational potential, $\phi \approx -GM_\mathrm{d}/R_\mathrm{d}$, we also obtain

$$\Delta\phi \approx \frac{GM_\mathrm{d}}{R_\mathrm{d}}\frac{\Delta R}{R} \qquad \Rightarrow \qquad S \approx y^2 \approx \frac{GM_\mathrm{d}}{\omega^2 R_\mathrm{d}}\frac{\Delta R}{R} \tag{7.4}$$

The product ρv can be estimated by considering that at L_1 the gas expands freely into the Roche lobe of the companion, so that the velocity is given by the local sound speed $c_\mathrm{s} = \sqrt{P/\rho}$. We can eliminate ρ by considering the equation of state, approximated by the polytropic relation $P = K\rho^\gamma$. This gives $c_\mathrm{s} = \sqrt{K\rho^{\gamma-1}}$ and hence $\rho \propto {c_\mathrm{s}}^{2/(\gamma-1)}$, so that

$$(\rho v)_{L_1} \propto {c_\mathrm{s}}^{\frac{\gamma+1}{\gamma-1}}$$

Finally, at L_1 the kinetic energy in the stream should equal the potential difference across it, i.e. $\frac{1}{2}v^2 = \Delta\phi$ which gives us $c_\mathrm{s} \approx v \propto \sqrt{\Delta R/R}$ from eq. 7.4. With both ρv and S now expressed in terms of $\Delta R/R$ we arrive at a dimensional relation between $\dot{M}$ and $\Delta R/R$:

$$\dot{M} \propto \left(\frac{\Delta R}{R}\right)^{\frac{3\gamma-1}{2\gamma-2}}$$

For stars with convective envelopes, i.e red giants or low-mass main-sequence stars, $\gamma = \frac{5}{3}$ and the value of the exponent equals 3. However, any other reasonable value of γ also yields a strong dependence of $\dot{M}$ on $\Delta R/R$.

A more detailed derivation applying Bernoulli's law to the gas flow through the nozzle around L_1 yields the following equation:

$$\dot{M} = -A\frac{M_\mathrm{d}}{P}\left(\frac{\Delta R}{R}\right)^3 \tag{7.5}$$

where M_d is the donor mass, P the orbital period and A is a numerical constant of order ∼10. This relation implies that (1) the mass transfer rate is highly sensitive to the radius excess, with a slowly increasing $\Delta R/R$ leading to strongly increasing $\dot{M}$, and (2) even a modest radius excess of say 10 % would lead to an enormous mass transfer rate and to the transfer of the entire donor mass in about a hundred orbits. In practice this means that for relatively slow, steady mass transfer, such as is observed semi-detached binaries, the donor only overfills its Roche radius by a small fraction. This can be seen by writing eq. (7.5) as

$$\frac{\Delta R}{R} \sim \left(\frac{\dot{M}}{M}P\right)^{1/3} = \left(\frac{P}{\tau_{\dot{M}}}\right)^{1/3} \tag{7.6}$$

where $\tau_{\dot{M}}$ is the timescale of mass transfer. For mass transfer occurring on the nuclear timescale or even on the thermal timescale of the donor (see Sect. 6.2.2) this yields $\Delta R/R_\mathrm{d} < 0.01$. Hence, unless mass transfer is much more rapid than the thermal timescale of the donor, it is a very good approximation to take $R_\mathrm{d} = R_\mathrm{L}$.

7.2 Orbital evolution during mass transfer

In Chapter 2 the orbital angular momentum per unit reduced mass, $l = J/\mu$, of a binary was derived. Hence the orbital angular momentum J of a binary is given by

$$J^2 = G\,\frac{{M_1}^2{M_2}^2}{M_1 + M_2}\,a(1-e^2). \tag{7.7}$$

In many cases the angular momentum stored in the rotation of the two stars is negligible compared to the orbital angular momentum, so that eq. (7.7) also represents the total angular momentum of the binary, to good approximation. By differentiating this expression we obtain a general equation for orbital evolution:

$$2\frac{\dot{J}}{J} = \frac{\dot{a}}{a} + 2\frac{\dot{M}_1}{M_1} + 2\frac{\dot{M}_2}{M_2} - \frac{\dot{M}_1 + \dot{M}_2}{M_1 + M_2} - \frac{2e\,\dot{e}}{1-e^2}. \tag{7.8}$$

In the case of Roche-lobe overflow in an already circularized binary, the last term is zero. The $\dot{J}$ term represents angular momentum loss from the binary, which can be due to spontaneous processes (such as gravitational wave radiation) or it can be associated with mass loss from the binary as a whole or from the component stars. In the latter case $\dot{J}$ is related to the $\dot{M}$ terms.

7.2.1 Conservative mass transfer

We first consider *conservative mass transfer*, in which the total mass and orbital angular momentum of the binary are conserved. In that case we can set

$$\dot{J} = 0 \qquad \text{and} \qquad \dot{M}_\mathrm{a} = -\dot{M}_\mathrm{d},$$

and eq. (7.8) reduces to

$$\frac{\dot{a}}{a} = 2\left(\frac{M_\mathrm{d}}{M_\mathrm{a}} - 1\right)\frac{\dot{M}_\mathrm{d}}{M_\mathrm{d}}. \tag{7.9}$$

Eq. (7.9) tells us that, because $\dot{M}_\mathrm{d} < 0$, the orbit shrinks ($\dot{a} < 0$) as long as $M_\mathrm{d} > M_\mathrm{a}$ and the orbit expands when $M_\mathrm{d} < M_\mathrm{a}$. In other words, the minimum separation for conservative mass transfer occurs when $M_\mathrm{d} = M_\mathrm{a}$. An explicit relation between the separation and the masses can be found by integrating eq. (7.9), or more directly from eq. (7.7) with $e = 0$:

$$M_\mathrm{d}^2\, M_\mathrm{a}^2\, a = \text{constant}, \qquad \text{or} \qquad \frac{a}{a_\mathrm{i}} = \left(\frac{M_\mathrm{d,i}}{M_\mathrm{d}}\frac{M_\mathrm{a,i}}{M_\mathrm{a}}\right)^2 \tag{7.10}$$

The index 'i' denotes the initial value. We can use Kepler's law to obtain similar relations between the rate of change of the orbital period $\dot{P}$ and the rate of mass transfer $\dot{M}_\mathrm{d}$, and between the period and masses directly:

$$\frac{\dot{P}}{P} = 3\left(\frac{M_\mathrm{d}}{M_\mathrm{a}} - 1\right)\frac{\dot{M}_\mathrm{d}}{M_\mathrm{d}}, \qquad \text{and} \qquad \frac{P}{P_\mathrm{i}} = \left(\frac{M_\mathrm{d,i}}{M_\mathrm{d}}\frac{M_\mathrm{a,i}}{M_\mathrm{a}}\right)^3 \tag{7.11}$$

The usefulness of the first equation is that it allows a determination of the mass transfer rate of observed semi-detached binaries, if the masses and the period derivative can be measured (and if the assumption of conservative mass transfer is valid). This is complicated by the fact that many binaries show short-term period fluctuations, while what is needed is the long-term average of the period derivative. However, for some binaries this long-term trend has been determined with reasonable accuracy.

7.2.2 Non-conservative mass transfer and mass loss

The assumption of conservation of total mass and angular momentum is a useful idealization, but it cannot be expected to hold in many circumstances. This is unfortunate because the situation becomes much more complicated and uncertain when mass and angular momentum loss from the binary have to be considered. Observationally there is evidence for both conservatively and non-conservatively evolving binaries, as we will discuss later. For now we will just derive some useful expressions for orbital evolution, in which mass and angular momentum loss are simply parameterized. These can also be applied

to the situation where one or both of the stars is losing mass by a stellar wind, in the absence of mass transfer.

Suppose that only a fraction β of the transferred mass is accreted by the companion star, so that

$$\dot{M}_\mathrm{a} = -\beta \dot{M}_\mathrm{d} \qquad \text{and} \qquad \dot{M}_\mathrm{a} + \dot{M}_\mathrm{d} = (1-\beta)\dot{M}_\mathrm{d}.$$

We also need to specify how much angular momentum is taken away by the matter that is lost from the binary. This can be parameterized in different ways, here we will take the specific angular momentum of the ejected matter to be γ times the specific angular momentum of the binary, i.e.

$$h_\mathrm{loss} \equiv \frac{\dot{J}}{\dot{M}_\mathrm{a} + \dot{M}_\mathrm{d}} = \gamma \frac{J}{M_\mathrm{a} + M_\mathrm{d}} \tag{7.12}$$

so that in eq. (7.8) we can replace the $\dot{J}$ term by

$$\frac{\dot{J}}{J} = \gamma(1-\beta)\frac{\dot{M}_\mathrm{d}}{M_\mathrm{d} + M_\mathrm{a}} \tag{7.13}$$

We can now derive an expression for the change in separation resulting from non-conservative mass transfer:

$$\frac{\dot{a}}{a} = -2\frac{\dot{M}_\mathrm{d}}{M_\mathrm{d}}\left[1 - \beta\frac{M_\mathrm{d}}{M_\mathrm{a}} - (1-\beta)(\gamma + \tfrac{1}{2})\frac{M_\mathrm{d}}{M_\mathrm{d} + M_\mathrm{a}}\right] \tag{7.14}$$

Note that the difficulty is in specifying β and γ, or rather, how these parameters depend on say the masses of the stars and on the details of the mass transfer process. We will address some of these problems later.

For some (still idealized) physical situations at least γ can be specified in terms of other quantities. Several 'modes' of non-conservative mass mass transfer can be considered:

Fast mode or Jeans mode If mass is lost from the donor star in the form of a fast isotropic wind, it will simply take away the specific orbital angular momentum of the donor in its relative orbit around the centre of mass, with $a_\mathrm{d} = a\, M_\mathrm{a}/(M_\mathrm{d} + M_\mathrm{a})$. The assumption of a fast wind implies that the ejected matter does not interact with the binary system, and a further assumption is that the physical size of the star is neglected so that it is treated as a point mass. Then the specific angular momentum of the wind matter is

$$h_\mathrm{loss} = a_\mathrm{d}^2\omega = \left(\frac{M_\mathrm{a}}{M_\mathrm{d} + M_\mathrm{a}}\right)^2 \sqrt{G(M_\mathrm{d} + M_\mathrm{a})\, a} \tag{7.15}$$

which can be verified to correspond to $\gamma = M_\mathrm{a}/M_\mathrm{d}$.

Isotropic re-emission Another physical situation that may arise is when mass is actually transferred to the companion by RLOF, but only part of this matter is accreted with the rest being ejected isotropically from the close vicinity of the accreting star. This can be the case when mass accretion drives an enhanced stellar wind from the accretor, or when the excess mass is ejected in the from of jets from a compact object. In that case $h_\mathrm{loss} = a_\mathrm{a}^2\omega$ which corresponds to $\gamma = M_\mathrm{d}/M_\mathrm{a}$.

Circumbinary ring The last situation, also sometimes called the 'intermediate mode', is when the mass that is lost is not ejected from the potential of the binary but forms a ring around the system. This may occur when a contact binary is formed and the critical potential surface corresponding to the outer Lagrangian point L_2 is reached. Mass will then be lost through L_2 without having enough energy to escape (see Fig. 6.1), and it may end up in a Keplerian orbit around the binary at some distance a_ring from the centre of mass. Then the specific angular momentum of such a ring will be

$$h_\mathrm{ring} = [G(M_\mathrm{d} + M_\mathrm{a})\, a_\mathrm{ring}]^{1/2} \tag{7.16}$$

which corresponds to

$$\gamma = \frac{(M_\mathrm{d} + M_\mathrm{a})^2}{M_\mathrm{d} M_\mathrm{a}} \sqrt{\frac{a_\mathrm{ring}}{a}} \tag{7.17}$$

A more detailed description of orbital evolution according to these modes, as well as for a combination of several modes, can be found in the paper by Soberman et al. (1997). Beware, however, that a different notation is used in that paper.

7.3 Stability of mass transfer

When Roche-lobe overflow starts, the stability of the mass transfer process and its consequences depend on (1) how the radius of the donor responds to the imposed mass loss, and (2) how the orbit (and therefore R_L) responds to mass transfer. Once mass transfer is initiated its development and outcome also depend on (3) the response of the companion star to the mass that is being transferred to it. We defer this last issue to a later section, and for now assume the accreting star is an inert point mass and consider only the effect on the donor star.

We can derive *stability criteria* for the onset of mass transfer by considering points (1) and (2). We do this by comparing the stellar radius to the Roche radius as a function of decreasing donor mass in the *R*-*M* diagram, as depicted schematically in Fig 7.1a. The diagram shows the Roche radius of the donor star for conservative mass transfer in a binary with total mass $2\,M_\odot$, and two examples of evolution tracks, for initial donor masses $1.0\,M_\odot$ (starting at point A) and $1.4\,M_\odot$ (starting at point D). The stars evolve vertically upwards in this diagram (nuclear expansion at constant mass) until the onset of RLOF

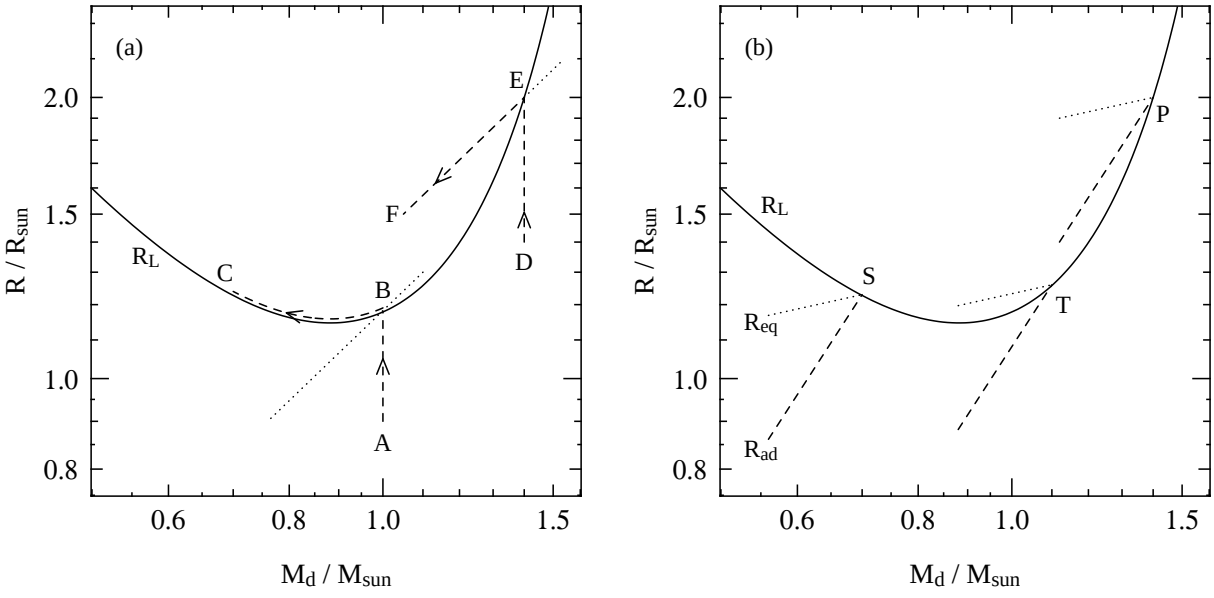

Figure 7.1. (a) Schematic behaviour of the Roche radius (solid line) and stellar radius (dashed lines, for two cases) as functions of the donor mass. The Roche radius curve is drawn for conservative mass transfer in a binary with total mass $2\,M_\odot$. The dotted lines show a fiducial stellar mass-radius relation, for the purpose of this example taken as $R \propto M$ (i.e. $\zeta_* = 1$). See test for discussion. (b) The solid curve is the same Roche radius as in panel a, but now the dashed and dotted lines indicate schematically the adiabatic (R_ad) and thermal-equilibrium (R_eq) responses of the donor to mass loss, respectively (for the purpose of illustration it is assumed that $\zeta_\mathrm{ad} = 1.5$ and $\zeta_\mathrm{eq} = 0.25$). Mass transfer starting at S, T and P correspond to stable, thermal-timescale and dynamically unstable mass transfer respectively, as discussed in the text.

at point B and E, respectively, when $R_d = R_L$. Upon mass loss the donor radius may behave as given by the dotted lines through points B and E. After a small amount of mass loss, $\delta M < 0$, we look at the quantity $\delta R = R_d - R_L$ and we can have either that $R_d \leq R_L$ ($\delta R \leq 0$, e.g. point B in Fig 7.1a) or $R_d > R_L$ ($\delta R > 0$, e.g. point E). In the first case, the donor detaches from its Roche lobe and it has to re-expand before RLOF can continue. Obviously this is the condition for stable mass transfer. In this case it is nuclear expansion that makes the donor continue to fill its Roche lobe and to drive mass transfer, and the stellar radius follows path B-C. In the second case ($\delta R > 0$) the mass transfer rate – which depends very strongly on $\delta R/R$ as shown in Sect. 7.1 – increases, leading to even more mass loss and a larger δR (path E-F in Fig 7.1a). This is a runaway situation, leading to unstable mass transfer. It thus appears that we have to compare the slope of the mass-radius relation, of both the stellar radius and the Roche radius. These slopes are expressed by the so-called mass-radius exponents,

$$\zeta_* \equiv \frac{d\log R_d}{d\log M}, \qquad \zeta_L \equiv \frac{d\log R_L}{d\log M}, \tag{7.18}$$

where $\zeta_* \geq \zeta_L$ implies stability and $\zeta_* < \zeta_L$ implies instability of RLOF. The situation is complicated, however, by the fact that stars react to perturbations (like mass loss) on two very different timescales.

If a star suddenly loses mass both its hydrostatic equilibrium and its thermal equilibrium will be disturbed. The star reacts by readjusting its structure and thereby its radius in order to recover equilibrium. Since hydrostatic readjustment happens on the star's dynamical timescale, which is much shorter than the Kelvin-Helmholtz timescale on which it readjusts thermally, the initial (dynamical) response to mass loss will be almost adiabatic. For the question of the *dynamical stability* of mass transfer we must thus consider the *adiabatic* response of the stellar radius to mass loss. This can be expressed as $(\delta R/R)_{ad} = \zeta_{ad}\,\delta M/M$, i.e. we define the adiabatic mass-radius exponent,

$$\zeta_{ad} \equiv \left(\frac{d\log R}{d\log M}\right)_{ad}. \tag{7.19}$$

The criterion for dynamical stability of mass transfer then becomes $\zeta_{ad} \geq \zeta_L$.

If this criterion is fulfilled, then the donor will shrink within its Roche lobe on a dynamical timescale and is able to recover hydrostatic equilibrium. In that case the slower thermal readjustment of the donor becomes relevant. On the Kelvin-Helmholtz timescale the star will attempt to recover the thermal equilibrium radius appropriate for its new mass $M + \delta M(< M)$, and the change in its equilibrium radius can be expressed as $(\delta R/R)_{eq} = \zeta_{eq}\,\delta M/M$ or

$$\zeta_{eq} \equiv \left(\frac{d\log R}{d\log M}\right)_{eq}. \tag{7.20}$$

If, in addition to $\zeta_{ad} \geq \zeta_L$, also $\zeta_{eq} \geq \zeta_L$ then the new equilibrium radius will be smaller than the Roche radius, and we have the condition for *secularly stable* mass transfer. In the intermediate case, $\zeta_{ad} \geq \zeta_L > \zeta_{eq}$, thermal readjustment of the donor keeps pushing it to overfill its Roche lobe. Mass transfer then occurs on the donor's thermal timescale as discussed below.

Based on the above stability considerations we can distinguish three cases of mass transfer, corresponding to different timescales, which are illustrated schematically in Fig 7.1b. (This classification is independent of the division into cases A, B and C discussed before!)

Case 1: stable mass transfer if $\zeta_L \leq \min(\zeta_{ad}, \zeta_{eq})$

This corresponds to mass transfer starting at point S in Fig 7.1b. The donor remains in thermal equilibrium, and continuing mass transfer is driven either by nuclear evolution of the donor (expansion, i.e. R_{eq} increases with time) or by orbital shrinkage due to angular momentum loss ($R_L$decreases). Mass transfer thus occurs on the nuclear timescale of the donor, or on the timescale for angular momentum loss, whichever is shorter.

Case 2: thermal-timescale mass transfer if $\zeta_{\rm ad} \geq \zeta_{\rm L} > \zeta_{\rm eq}$

Mass transfer is dynamically stable, but driven by thermal readjustment of the donor. This corresponds to mass transfer starting at point T in Fig 7.1b. Initially the mass transfer rate increases, but then saturates at a value determined by the donor's thermal timescale:

$$\dot{M}_{\rm max} \approx -M_{\rm d}/\tau_{\rm KH,d} \tag{7.21}$$

This case is sometimes called 'thermally unstable' mass transfer but this is misleading: despite the thermal disequilibrium of the donor, mass transfer is stable and *self-regulating*. If $\dot{M}$ were smaller than eq. (7.21) the donor would be allowed to expand to regain equilibrium, leading to an increasing mass transfer rate. On the other hand if $\dot{M}$ were much larger the donor would react almost adiabatically and shrink inside its Roche lobe. The radius excess $\delta R/R$ adjusts itself to maintain the thermal-timescale mass loss rate. As shown in Sect. 7.1, this implies $\delta R/R < 0.01$. Hence also in this case, the donor radius closely follows the Roche radius, but $R_{\rm d} < R_{\rm eq}$.

Case 3: dynamically unstable mass transfer if $\zeta_{\rm L} > \zeta_{\rm ad}$

This corresponds to mass transfer starting at point P in Fig 7.1b. The adiabatic response of the donor is unable to keep it within its Roche lobe, leading to ever-increasing mass-transfer rates. As discussed above this is an unstable, runaway situation. Detailed calculations show that mass transfer accelerates to a timescale in between the thermal and dynamical timescale of the donor. This has dramatic effects on the evolution of the binary, probably leading to a common-envelope situation (Sect. 10.2).

For these criteria to be of practical use, we need to consider how the various ζ's depend on the properties of the binary system and on the mass and evolution state of the donor.

7.3.1 Response of the Roche radius to mass loss

The example shown in Fig 7.1 indicates that the reaction of the Roche radius depends primarily on the binary mass ratio. This can be easily shown for the case of conservative mass transfer, for which (see Exercise 7.1)

$$\zeta_{\rm L} = 2.13q - 1.67, \qquad \text{for } q = M_{\rm d}/M_{\rm a} < 10. \tag{7.22}$$

The important consequence of this expression is that the stability criteria for mass transfer can be rewritten in terms of a critical mass ratio (see § 7.3.3 below). However, it is important to realize that $\zeta_{\rm L}$ can take on different values for non-conservative mass transfer, i.e. it depends on the mode of mass and angular-momentum loss, as well as on the mass ratio. For a particular mode, such as those discussed in Sect. 7.2.2, the dependence of $\zeta_{\rm L}$ on mass ratio can be derived (see the article by Soberman et al., 1997).

7.3.2 Response of the stellar radius to mass loss

The adiabatic response of a star to mass loss, and hence the value of $\zeta_{\rm ad}$, depends critically on the structure of its envelope, in particular on whether the envelope is convective or radiative. Detailed calculations show that stars with radiative envelopes shrink rapidly in response to mass loss (i.e. $\zeta_{\rm ad} \gg 0$), while stars with convective envelopes tend to expand or keep a roughly constant radius ($\zeta_{\rm ad} \lesssim 0$).

We can make this plausible by recalling the criterion for convection to occur. If a gas element is displaced upwards adiabatically from its equilibrium position, while maintaining pressure equilibrium with its surroundings, it will experience an upward buoyancy force if its density is smaller than that of its surroundings. The envelope is then unstable to convective motions, which efficiently redistribute energy so as to make the envelope structure nearly adiabatic. This means that $P \propto \rho^{\gamma_{\rm ad}}$, i.e. the density

within a convective envelope falls off with pressure as $\rho \propto P^{1/\gamma_{\rm ad}}$. On the other hand, if the envelope is stable against convection, the density gradient must necessarily be steeper than adiabatic in order for the buoyancy force on a displaced gas element to restore it to its original position. This means that radiative envelopes are more centrally concentrated than convective envelopes, and have relatively low density in the outer layers. When the outermost layers of a star are suddenly removed by mass loss, the layers below it are decompressed and will expand adiabatically to restore pressure equilibrium. For a convective envelope that is already adiabatically stratified, we may therefore expect that the density distribution (measured at constant pressure) will remain the same, and the star will therefore occupy about the same volume when hydrostatic equilibrium is restored. In other words, $R_{\rm ad}$ is insensitive to mass loss. On the other hand, the steeper initial density profile in a radiative envelope means that, first of all, the layers exposed by mass loss lie deeper within the star. After adiabatic expansion, the outer layers will furthermore have a higher density when measured at constant pressure. Therefore when hydrostatic equilibrium is restored, a star with a radiative envelope will occupy a *smaller* volume and have a smaller radius.

This expectation is borne out by more detailed considerations. For an ideal monatomic gas, $\gamma_{\rm ad} = \frac{5}{3}$, and a convective envelope behaves like an $n = \frac{3}{2}$ polytrope. Stars whose entire structure is described by an $n = \frac{3}{2}$ polytrope, such as white dwarfs and completely convective stars, follow a mass-radius relation $R \propto M^{-1/3}$, i.e. they expand upon mass loss and $\zeta_{\rm ad} = -\frac{1}{3}$. This is relevant for low-mass main-sequence stars with $M \lesssim 0.35\,M_\odot$ which are completely convective. Evolved stars on the red giant branch have deep convective envelopes and a dense core, these can be described by so-called condensed polytropes. The response of such models to mass loss was studied by Hjellming & Webbink (1987) who found $\zeta_{\rm ad}$ to increase with the fractional mass of the dense core, turning positive for $M_{\rm c} > 0.2M$; see Fig. 1 of Soberman et al. (1997) who also provide a convenient fitting formula, eq. (60). To summarize, stars with deep convective envelopes respond to mass loss by either expanding or keeping their radius roughly constant. This has important consequences for mass transfer from red giants.

The equilibrium radius response to mass loss also depends on the evolution state of the donor, but in a different way. For homogeneous stars, i.e. stars on the zero-age main sequence, $R_{\rm eq}$ is simply given by their mass-radius relation. Hence for upper ZAMS stars ($M \gtrsim 1\,M_\odot$) we have $\zeta_{\rm eq} \approx 0.6$ and for low-mass ZAMS stars ($M \lesssim 1\,M_\odot$) $\zeta_{\rm eq} \approx 1.0$. However for stars that are more evolved, and have a non-homogeneous composition profile, we cannot simply apply the MS mass-radius relation. We need to consider the response on a timescale that is much slower than thermal, so that the star remains in TE, but faster than the nuclear timescale, so that the composition profile does not change. The effect of a non-homogeneous composition is to make stars expand rather than contract in response to mass loss, as is borne out by detailed calculations. Hence $\zeta_{\rm eq} \lesssim 0$ for fairly evolved MS stars. Detailed calculations also show that for stars in post-MS phases, the equilibrium radius is insensitive to the total stellar mass, hence $\zeta_{\rm eq} \approx 0$. On the other hand, for low-mass red giants the radius depends strongly on the *core* mass, see Sect. 6.2.3.

Finally, for white dwarfs the response is again given by their mass-radius relation, i.e. $\zeta_{\rm eq} = -\frac{1}{3}$. For these degenerate configurations there is no distinction between the adiabatic and thermal response.

7.3.3 Consequences for binary evolution

The stability criteria discussed above translate, with the use of eq. (7.22), into critical mass ratios for the stability of (conservative) mass transfer. Since the initial mass ratio $q = M_{\rm d}/M_{\rm a} > 1$, the initial value of $\zeta_{\rm L}$ is always > 0.46. Stars with deep convective envelopes, i.e. red giants and red supergiants, have $\zeta_{\rm ad} \lesssim 0$, so the first stage of mass transfer from such donors will always be dynamically unstable. Comparison with Fig 6.2 shows that Case C mass transfer is always expected to be dynamically unstable, as well as Case B mass transfer in low-mass binaries and late Case B mass transfer in intermediate-mass

binaries, with RLOF starting on the first giant branch. Dynamically unstable mass transfer can only be avoided in these binaries if stellar-wind mass loss reduces the donor mass to well below the accretor mass, so that $q \lesssim 0.8$ when RLOF starts.

For donors with radiative envelopes, having $\zeta_{\rm ad} \gg 0$, RLOF will only be dynamically unstable if the donor is much more massive than the accretor. For $q \lesssim 4$ mass transfer is dynamically stable and usually occurs on the thermal timescale, since for practically all stars $\zeta_{\rm eq} \lesssim 0$. Only if the donor fills its Roche lobe very close to the ZAMS ($\zeta_{\rm eq} \approx 0.6 - 1.0$) in a very close binary with nearly equal masses, can one expect stable (nuclear-timescale) mass transfer. Therefore thermal-timescale mass transfer should occur in most Case A binaries, as well as early Case B binaries of intermediate and high mass with periods such that mass transfer occurs during the Hertzprung-gap expansion of the donor.

Exercises

7.1 Using the approximate expression (6.2) for the Roche-lobe radius of the donor, show that for conservative mass transfer the rate of change of $R_{\rm L}$ is given by

$$\frac{\dot{R}_{\rm L}}{R_{\rm L}} = \left(2.13\frac{M_{\rm d}}{M_{\rm a}} - 1.67\right)\frac{\dot{M}_{\rm d}}{M_{\rm d}} \tag{7.23}$$

and that $R_{\rm L}$ has a minimum for $M_{\rm d} \approx 0.78 M_{\rm a}$.

7.2 β Lyrae is a semi-detached eclipsing binary in which the orbital period has been observed to change over the last 100 years. The observed ephemeris (the time of primary eclipse as a function of orbital cycle) is quite accurately fitted by a parabolic expression:

$$T_{\rm prim.eclipse}({\rm d}) = {\rm JD}2408247.966 + 12.913780\,E + 3.87196 \times 10^{-6}\,E^2$$

where E counts the number of eclipses.

(a) Derive the orbital period of β Lyr and the rate of change of its orbital period.

(b) From the radial velocity variations the masses of the components have been measured as $M_1 \sin^3 i = 12.94 \pm 0.05\,M_\odot$ and $M_2 \sin^3 i = 2.88 \pm 0.10\,M_\odot$. The inclination is not accurately measured, however. Assuming conservative mass transfer is taking place, calculate the mass transfer rate and estimate its uncertainty.

7.3 Show that in a binary system in which one star is losing mass in a fast, isotropic stellar wind, the separation relates to the total binary mass as

$$a\,(M_1 + M_2) = \text{constant} \tag{7.24}$$

if the finite dimensions of the star are ignored (i.e. it is treated as a point mass).

This result implies that if one or both stars are losing mass, the binary separation increases (inversely with total mass) even though the angular momentum decreases.

7.4 Derive the following expression for the mass transfer rate for stable (nuclear-timescale) mass transfer, in terms of the mass mass-radius exponents $\zeta_{\rm L}$ and $\zeta_{\rm eq}$ and the rate at which the stellar (equilibrium) radius would change in the absence of mass loss, $(\partial R_{\rm eq}/\partial t)_M$:

$$\dot{M}_{\rm d} = -\frac{M_{\rm d}}{\zeta_{\rm eq} - \zeta_{\rm L}}\left(\frac{\partial \ln R_{\rm eq}}{\partial t}\right)_M \tag{7.25}$$

(Hint: write $\dot{R} = dR/dt$ in terms of the partial derivatives with respect to t and M, and use the condition that the donor star just keeps filling its Roche lobe exactly, which is accurate to $\lesssim 0.1\%$.)

Verify that this indeed gives reasonable mass transfer rates if the condition for stable mass transfer is fulfilled.

Chapter 8

Conservative binary evolution

In the previous chapter we came to the conclusion that when mass transfer starts while the donor still has a radiative envelope, i.e. it first fills its Roche lobe on the main sequence or the Hertzsprung gap (case A or early case B), and if the initial mass ratio $M_1/M_2 \lesssim 4$, then mass transfer should occur on the donor's thermal timescale. Although this can imply quite high rates of mass transfer, the process itself is self-regulating and stable. Under such circumstances it is not unreasonable to make the assumption of conservative mass transfer (§ 7.2.1), because the matter that is transferred through the inner Lagrangian point does not have sufficient energy to escape from the companion's Roche lobe. In this chapter we therefore consider conservative binary evolution according to case A and case B.

Whether mass transfer really is conservative depends on the response of the companion star to accretion. This constitutes a still unsolved problems in the evolution of close binaries: how much mass and angular momentum are lost from a binary system during phases of stable Roche-lobe overflow, and how does this depend on the masses and orbital parameters of the binary. We will address this question in Sect. 8.3 of this chapter.

8.1 Case A evolution and the Algol systems

In short-period binaries evolving according to case A, the first phase of mass transfer can usually be divided into a rapid phase on the thermal timescale of the primary, followed by a slow phase on the much longer nuclear timescale. This is illustrated in Fig. 8.1, which shows the result of a detailed evolution calculation for the primary component in a binary with initial masses 10.0 and 8.9 $M_\odot$ and an initial period $P = 2.2$ d. The M-R diagram can be compared to Fig. 7.1 in the previous chapter. The rapid phase of mass transfer, starting at point B, continues until the primary has regained thermal equilibrium, i.e. when its equilibrium radius becomes smaller than its Roche radius (point C). By this time the primary has become the less massive star in the binary, in other words the mass ratio has been reversed. Further mass transfer is driven by expansion of the primary and takes place on the nuclear timescale, until the primary has reached the end of its main-sequence phase (point D).

For the same binary, Fig. 8.2 shows the evolution of both components. The binary is detached during phase A–B. During the rapid mass-transfer phase (B–C) both stars are out of thermal equilibrium: the primary is somewhat less luminous due to mass loss, while the secondary is somewhat more luminous as a result of accretion (see §8.3). At point C both stars have regained thermal equilibrium, and phase C–D is a long-lived phase of nuclear-timescale mass transfer. The secondary has a luminosity and radius appropriate for a MS star of its increased mass, but the now less massive primary is over-luminous for its mass, and has a larger radius than the secondary.

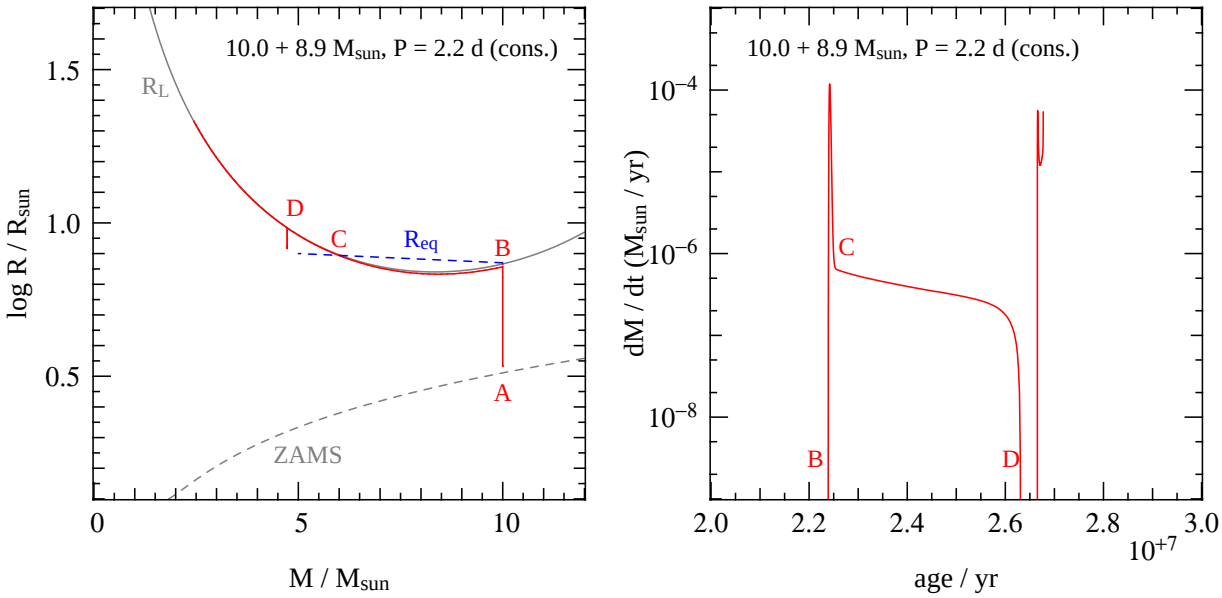

Figure 8.1. Mass-radius diagram of the primary star in a massive binary with initial parameters 10.0 + 8.9 $M_\odot$, P = 2.2 d, with metallicity Z = 0.004. The right diagram shows the corresponding mass transfer rate as a function of time. The primary expands during its main-sequence evolution from point A to point B, when it fills its Roche lobe. The dashed line indicates the equilibrium radius, which is larger than the Roche radius between B and C. This corresponds to a phase of rapid, thermal-timescale mass transfer. At C the primary regains thermal equilibrium, and further mass transfer (C-D) is driven by expansion and takes place on the nuclear (MS) timescale. Point D corresponds to the end of the MS phase of the primary, when it detaches from its Roche lobe for a short time. During H-shell burning the primary re-expands, giving rise to further mass transfer past point D (on the much faster expansion timescale associated with crossing the Hertzsprung gap).

Table 8.1. Some observed Algol-type binaries. Masses, radii and luminosities are given in solar units.

name	spectra	P (d)	M_1	M_2	R_1	R_2	$\log L_1$	$\log L_2$
V Pup	B2 + B1V	1.45	9	17	5.3	6.3	3.85	4.20
TT Aur	B6 + B3	1.33	5.4	8.1	4.2	3.9	3.21	3.71
U Her	B8-9 + B2V	2.05	2.9	7.6	4.4	5.8	2.49	3.68
Z Vul	A2III + B3V	2.45	2.3	5.4	4.5	4.7	2.07	3.30
U CrB	G0III + B5.5V	3.45	1.46	4.98	4.94	2.73	1.43	2.51
β Per (Algol)	G8III + B8V	2.87	0.8	3.7	3.5	2.9	0.65	2.27
V356 Sgr	A2III + B4V	8.90	4.7	12.1	14	6		

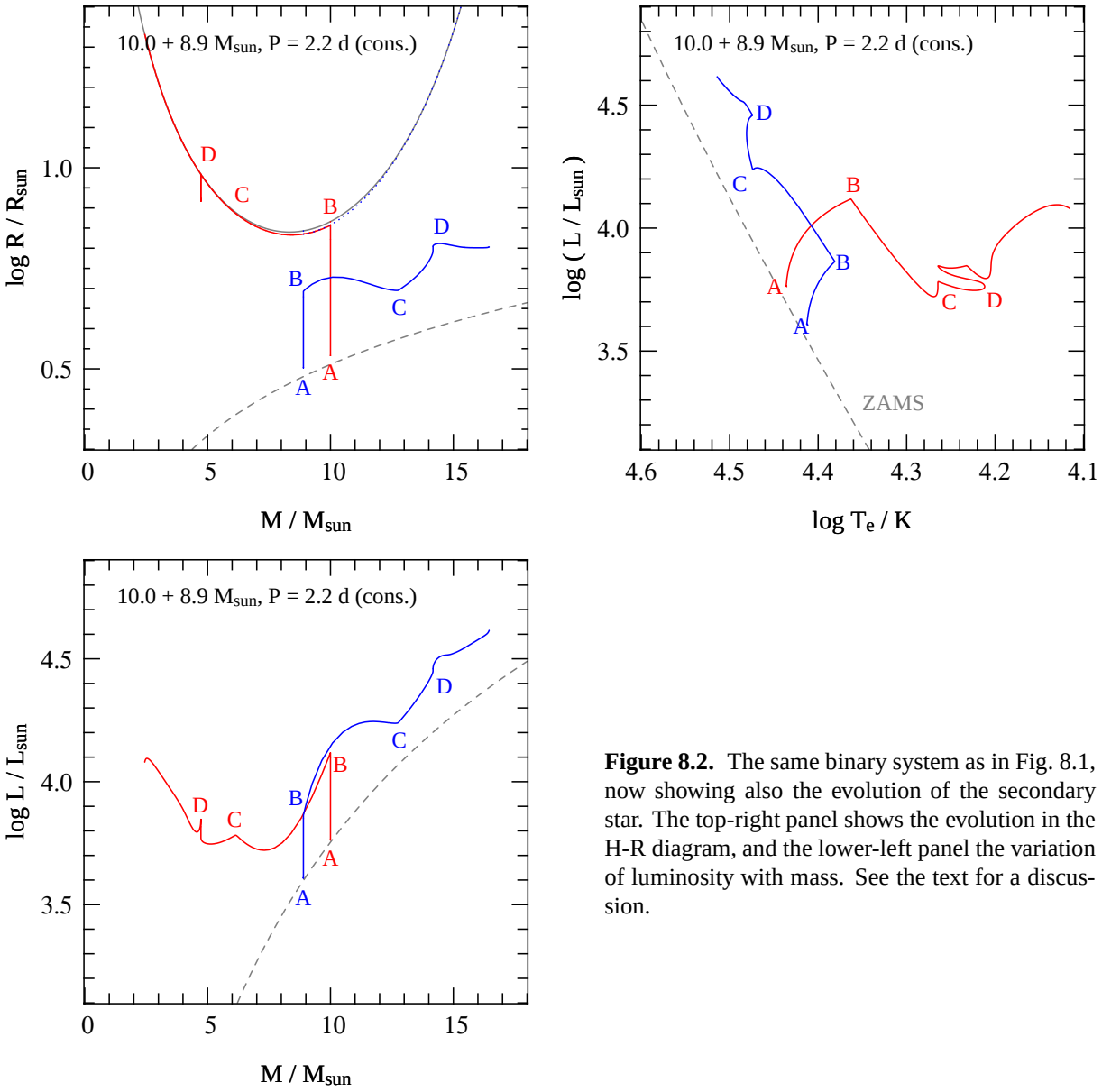

Figure 8.2. The same binary system as in Fig. 8.1, now showing also the evolution of the secondary star. The top-right panel shows the evolution in the H-R diagram, and the lower-left panel the variation of luminosity with mass. See the text for a discussion.

These properties are typical of many observed semi-detached binaries, so-called Algol-type binaries. Table 8.1 lists observed properties of several Algol-type systems. The primary (*1) is now filling its Roche lobe and is interpreted as the originally most massive star. The secondary (*2) is currently the more massive and more luminous star, but is often smaller in radius than the primary. Many such binaries are known, which is in accordance with the fact that the semi-detached phase of slow mass transfer lasts for the remaining main-sequence lifetime of the primary. The first group of six systems in Table 8.1 are interpreted as undergoing slow case A mass transfer. The last system is an example of a group of rarer, wider semi-detached systems that may be undergoing case B mass transfer (see § 8.2).

Nelson & Eggleton (2001) computed a large grid of conservative case A evolution models, covering the entire parameter space in masses and orbital periods. They compared their models to observed Algol binaries. This paper provides interesting background reading.

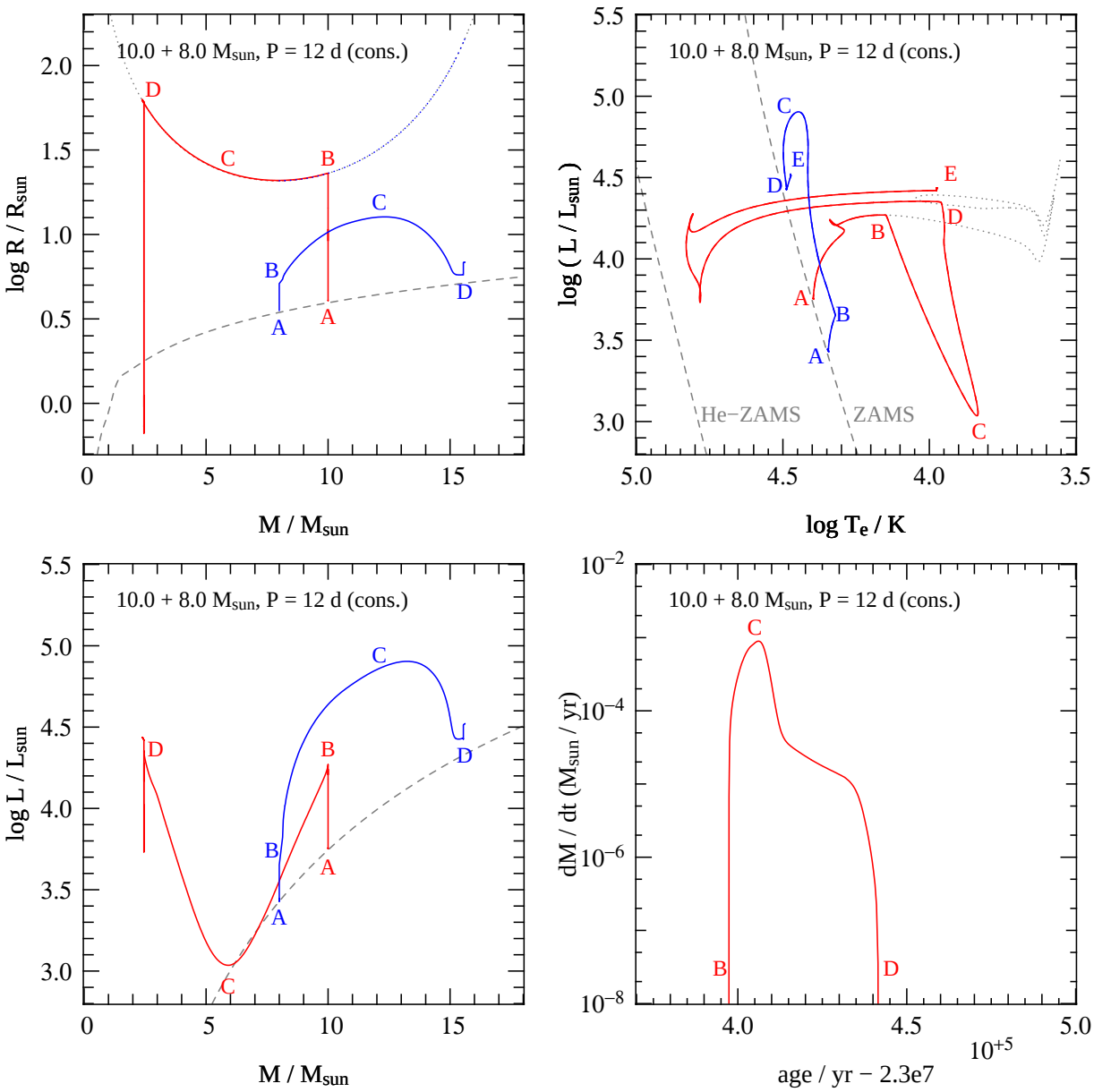

Figure 8.3. Conservative evolution of a binary of 10.0 + 8.0 $M_\odot$, P = 12 d, undergoing case B mass transfer. Panels are similar to those in Fig 8.2, with the bottom-right panel showing the mass transfer rate as a function of time. Note the expanded scale: the entire mass-transfer phase (B-D) lasts < 2% of the preceding MS lifetime. Point C corresponds to the maximum mass-transfer rate, coinciding with the minimum in the primary's luminosity and the maximum in the secondary's luminosity.

8.2 Case B evolution

Early case B mass transfer in intermediate-mass and massive binaries, with periods ranging from a few days to ~100 days, depending on the primary mass, is in many respects similar to case A. Since the donor's envelope is radiative mass transfer starts with a rapid, thermal-timescale phase during which the mass ratio is reversed. An important difference is that since the primary is more extended and therefore has a shorter thermal timescale (§ 6.2.2) compared to case A, the mass transfer rates during the rapid

Table 8.2. Some observed post-RLOF binaries. Masses and radii are given in solar units.

name	spectra	P (d)	M_1	M_2	R_1	R_2
CQ Cep	WN7 + O6	1.64	24	30	8.8	7.9
V398 Car	WN4 + O4-6	8.26	19	37		
GP Cep	WN6/WC + O3-6	6.69	15	27		
CV Ser	WC8 + O8-9	29.7	13	27		
V444 Cyg	WN5 + O6	4.21	9.3	28	2.9	8.5
ϕ Per	HeI em + B1IIIe	127	1.15	9.3	1.3:	5.5–8

phase are correspondingly higher. Furthermore the primary is itself in a rapid phase of evolution: while crossing the Hertzsprung gap it is out of thermal equilibrium and expands on the timescale at which its core contracts. As a consequence, after mass-ratio reversal mass transfer continues on the expansion timescale of the primary, only slightly slower than the thermal timescale. Therefore there is no 'slow' phase of mass transfer as in case A binaries. Mass transfer continues at a fairly high rate until most of the envelope has been transferred, as illustrated in Fig. 8.3. The evolution track describes a loop in the H-R diagram during the mass transfer phase, points B-D, with the maximum transfer rate coinciding with the minimum in luminosity of the primary at point C. The decrease in luminosity during mass transfer is caused by the strong thermal disequilibrium of the primary: as described in § 7.3 a radiative donor star shrinks in response to mass loss and has to re-expand to regain thermal equilibrium. This requires the absorption of gravitational energy, so that the surface luminosity during thermal-timescale mass transfer is (much) smaller than the nuclear luminosity provided by the H-burning shell.

When helium is ignited in the core (pomt D) mass transfer stops: the primary contracts and detaches from its Roche lobe. This happens when the primary is almost reduced to its bare helium core, with only a thin H-rich layer. The primary moves to a position close to the helium main-sequence in the H-R diagram. From single-star evolution models of intermediate-mass and massive stars, the mass of the helium core after the main sequence (when the star crosses the Hertzsprung gap) is well approximated by

$$M_{\rm core}/M_\odot = 0.10\,(M_{\rm i}/M_\odot)^{1.4}, \tag{8.1}$$

where $M_{\rm i}$ is the initial mass. If we make the assumption of conservative mass transfer, we can use this relation to either (1) predict the outcome of case B mass transfer, or (2) trace back the evolution of an observed binary that we believe to have undergone case B mass transfer.

Since the mass-transfer phase in case B binaries is very short compared to case A binaries, observational counterparts are rare. Indeed the vast majority of observed Algol-type binaries have short periods, $P < 10$ d. One likely example of a binary currently undergoing case B mass transfer is β Lyrae which we encountered in Exercise 7.2. On the other hand, the remnants of case B mass transfer are in a long-lived phase of evolution: these are binaries consisting of the almost bare helium-burning core of the primary and a more massive main-sequence star. Conservative mass transfer will have widened their orbits significantly. Observed counterparts of this evolution phase among massive systems are the WR+O binaries, consisting of a Wolf-Rayet star and a massive O star. Some examples are given in Table 8.2. Among intermediate-mass binaries on the other hand, not many counterparts are known. This is probably a selection effect: the He star is much hotter and less luminous than its companion, so it will be optically much fainter. Furthermore its low mass and the wide orbit after conservative mass transfer imply that the orbital velocity of the main-sequence star is undetectably small. The best candidate for this phase of evolution is the binary ϕ Persei: a binary with $P_{\rm orb} = 127$ d consisting of a B1e main sequence star and a He emission-line object, presumably a naked He-burning star (Gies et al., 1998, see Table 8.2).

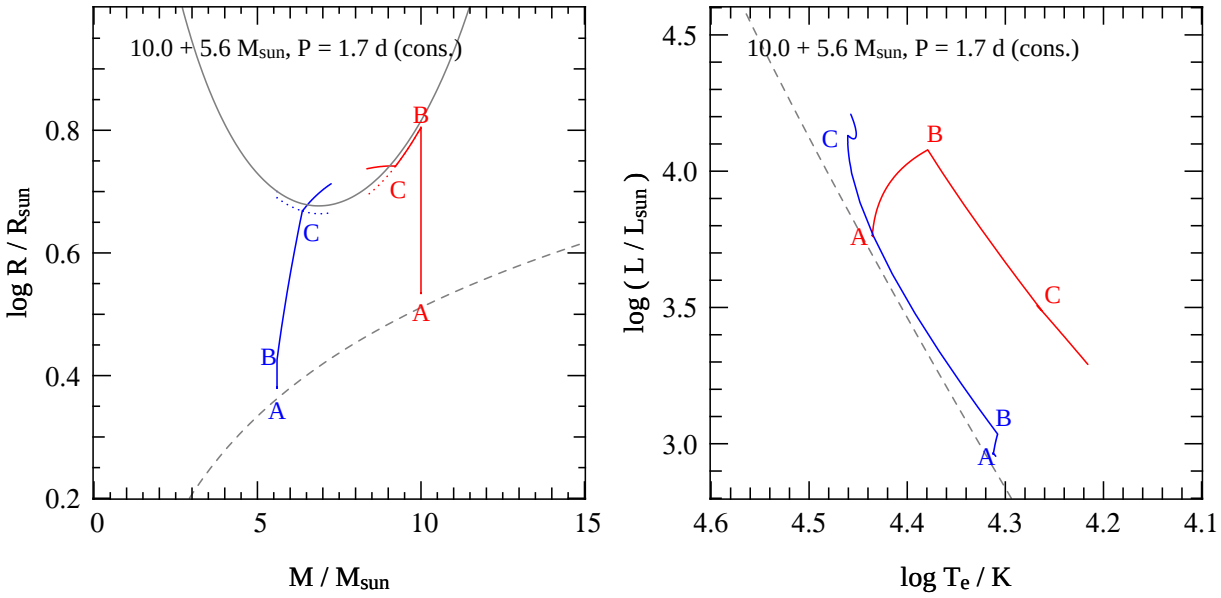

Figure 8.4. Similar to Fig 8.2, but for a binary with a more extreme initial mass ratio. The large difference in thermal timescales between the primary and secondary causes the secondary to become highly over-luminous and expand in response to accretion. As a result the secondary fills its Roche lobe during rapid mass transfer, after only a small amount of accretion, and a contact binary is formed at point C.

8.3 The response of the mass gainer

The mass transfer stream from the donor will follow a more-or-less ballistic orbit, reaching a minimum distance $d_{\rm min}$ from the center of mass of the companion which scales with the orbital separation. The stream hits the accreting star directly if $R_{\rm a} > d_{\rm min}$, otherwise it continues in its orbit and collides with itself, forming an accretion disk around the companion. This latter possibility occurs in relatively wide orbits, compared to the companion's radius. As a consequence not only mass but also angular momentum is transferred to the companion. Accretion onto the companion star therefore has three important consequences for its structure and evolution[1]:

Thermal readjustment and expansion

The secondary star has to adjust its structure to the added mass. The main effect of accretion is the compression of underlying layers which releases gravitational energy. If this energy release is larger than the luminosity of the star it will be brought out of thermal equilibrium. This is the case if accretion takes place on a timescale shorter than the accretor's Kelvin-Helmholtz timescale. One may then expect the reverse of the effect of rapid mass loss on the donor star (§ 7.3): accretion onto a star with a convective envelope makes it shrink, while accretion onto a star with a radiative envelope causes it to expand. This is indeed borne out by detailed calculations.

During the first mass transfer phase the thermal timescale of the secondary is longer than that of the donor, so that the accretor will be brought out of thermal equilibrium. This makes it brighter than the main-sequence luminosity appropriate for its mass, and for sufficiently high accretion rates, also causes

[1]One should also consider the kinetic energy of the stream but this is probably dissipated locally and radiated away, either in the accretion disk and its boundary layer, or in a 'hot spot' where the stream hits the stellar surface, and therefore does not add to the energy budget of the accreting star.

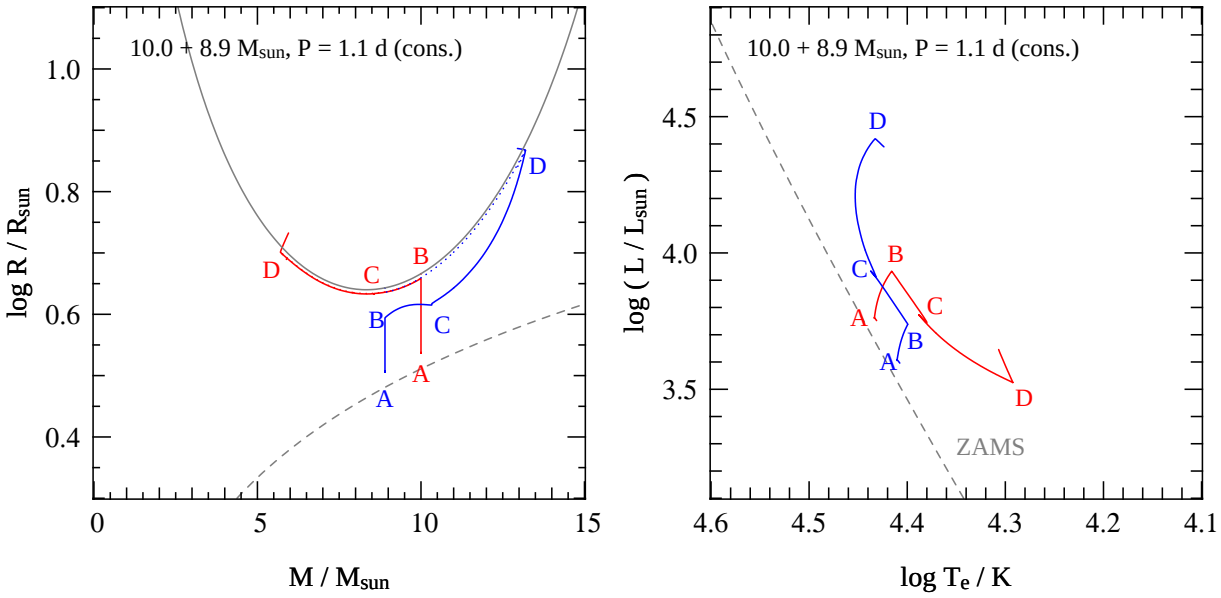

Figure 8.5. Similar to Fig 8.2, but for a binary with a smaller orbital period. During rapid mass transfer (BC) the secondary remains close to thermal equilibrium, but during the subsequent slow mass transfer (C-D) its evolution speeds up and eventually overtakes that of the primary. As a result a contact binary is formed at point D.

substantial expansion of the star over its main-sequence radius (see Fig. 8.3, point C on the evolution track of the secondary). As a consequence the secondary may fill its own Roche lobe and a contact binary can be formed. An example of this is given in Fig. 8.4.

Spin-up of the accreting star

The matter that is transferred to the secondary carries a significant amount of angular momentum, especially if it passes through an accretion disc. This can bring the secondary to break-up rotation after accreting only about 10 % of its original mass (Packet, 1981). The secondary then has to get rid of some, or most, of its angular momentum before further accretion can take place. Hence this 'angular momentum catastrophe' potentially limits the amount of accretion much more than the effect of expansion discussed above. Tidal interaction with the companion can transfer spin angular momentum back into the orbit, thus preventing critical rotation, but only in very close binaries with periods less than a few days. Another way by which the accreting star may get rid of its angular momentum is by mass loss. In massive binaries at least, the (normally weak) stellar wind may be enhanced enormously when the star is rotating very close to critical; this enhanced wind takes away the excess angular momentum. This process necessarily leads to non-conservative mass transfer, and a small value of the mass transfer efficiency parameter β (discussed in §7.2.2).

Despite these theoretical considerations, it appears that close-to-conservative mass transfer *does* occur in practice even in systems that are too wide for tidal interaction to be important, and of too low mass for stellar winds to be significant. A case in point is the Be-star binary ϕ Per discussed above, whose wide orbit and small mass ratio are indicative of conservative mass transfer. The secondary component is a rapidly rotating Be star, presumably as a result of spin-up by mass transfer. The same process is responsible for the formation of the Be stars seen as companions in many high-mass X-ray binaries. If the component masses in ϕ Per had been a factor ~2 higher, it would have been the perfect progenitor system of such a Be/X-ray binary.

Rejuvenation

If mass transfer is indeed (close to) conservative then the mass of the secondary is increased significantly. This has two effects on its further evolution. First, the added mass causes its convective core to grow in mass, mixing in fresh fuel from outer layers into the nuclear-burning zone in the center. This process is called rejuvenation, since it has the effect of extending the main-sequence lifetime of the secondary.[2] This can be seen in Fig 8.3 where after mass transfer (point D) the secondary is closer to the ZAMS than at the start (point B). The rejuvenation effect is counteracted, however, by the fact that its nuclear timescale (which scales approximately with $M^{-2.8}$, § 6.2.2) becomes much shorter. The combined result is that the secondary can overtake the evolution of the primary under some circumstances. An example of this is given in Fig. 8.5.

8.3.1 Formation of contact binaries

A number of studies have investigated for which binary parameters the secondary can evolve into contact (Pols, 1994; Nelson & Eggleton, 2001; Wellstein et al., 2001). In these binary evolution calculations the spin-up of the secondary was neglected. The results indicate that contact arises in three different circumstances:

1. During rapid (thermal timescale) RLOF, either in case A or early case B. This occurs for $M_1/M_2 > q_{\rm cr}$, where $q_{\rm cr}$ is in the range $1-2$ depending on primary mass. In this case the thermal timescale of the accretor is much longer than the accretion timescale, so that it swells up quickly and fills its Roche lobe after accreting only a small amount of mass (e.g. Fig. 8.4).

2. During the slow (nuclear timescale) phase RLOF in case A after the mass ratio is reversed. For very short $P_{\rm orb}$ the nuclear evolution of the secondary can then overtake that of the primary (e.g. Fig. 8.5). The ensuing contact stage may be quite long-lived given that massive contact binaries are not uncommon, but the evolution of such systems is not well understood.

3. During the late phase of RLOF in case B for fairly long periods, when $\dot{M}$ accelerates as the envelope of the donor becomes partly convective. In this case, a contact binary is formed after substantial mass accretion has already taken place.

Based on the above, regions in parameter space (q_0 and P_0) where contact is avoided can be identified. Examples of this can be found in the papers cited above.

Neglecting other effects, one might expect conservative mass transfer in those systems that avoid contact altogether, and up to the point where contact is reached in the other cases. However, the further evolution of contact binaries is highly uncertain, and how much mass and angular momentum these systems lose are still open questions. It seems likely that a case A contact binary must eventually merge to a single star, while in a case B situation the contact binary may quickly evolve into a common-envelope configuration (§ 10.2).

Exercises

8.1 Consider the binary depicted in Fig. 8.1. Verify that the rapid mass-transfer phase (B–C) indeed takes place on the thermal timescale of the donor, and that the slow phase (C–D) takes place on the nuclear timescale of the donor. Assume typical values for a $10\,M_\odot$ main-sequence star.

[2] Not all detailed evolution models of accreting stars show such rejuvenation, it depends on the uncertain mixing efficiency in semi-convective layers.

8.2 We have seen that for case B mass transfer in intermediate-mass or massive binaries, almost the entire envelope of the donor star is transferred and the remnant is the almost bare helium core of the donor. For a binary system with masses $4 + 3\,M_\odot$, see Exercise 6.3, calculate the masses of the components after conservative case B mass transfer. Subsequently calculate the range of final orbital periods after conservative case B mass transfer, taking into account for which systems you may reasonably expect the conservative assumption to hold.

8.3 Compare the outcome of case B mass transfer for a primary mass of $4\,M_\odot$ (previous exercise) with that of $10\,M_\odot$ and $40\,M_\odot$, assuming the same initial mass ratio of 0.75, in terms of (a) the final mass ratio and (b) the ratio of final to initial orbital period.

8.4 Assuming the He-star + Be-star system ϕ Persei (see Table 8.2) formed by conservative case B mass transfer, calculate the initial masses and orbital period of the binary. Is this consistent with the case B assumption?